



Surface plasmon resonance immunosensor for bacteria detection

H. Baccar^{a,b}, M.B. Mejri^{a,c}, I. Hafaiedh^{a,b}, T. Ktari^a, M. Aouni^c, A. Abdelghani^{a,b,*}

^a Nanotechnology Laboratory, INSAT, Centre Urbain Nord, 1080 Charguia Cedex, Tunisia

^b Unité de recherche de Physico-chimie des Matériaux Polymères, IPEST, 2070 La Marsa, Tunisia

^c Laboratoire des maladies transmissibles et substances biologiquement actives (LR99ES27), Faculté de Pharmacie, 5000 Monastir, Tunisia

ARTICLE INFO

Article history:

Received 5 March 2010

Received in revised form 28 May 2010

Accepted 28 May 2010

Available online 4 June 2010

Keywords:

SPR

Biofunctionalization

Immunosensor

Gold nanoparticles

ABSTRACT

This work describes an approach for the development of two bacteria biosensors based on surface plasmon resonance (SPR) technique. The first biosensor was based on functionalized gold substrate and the second one on immobilized gold nanoparticles. For the first biosensor, the gold substrate was functionalized with acid–thiol using the self-assembled monolayer technique, while the second one was functionalized with gold nanoparticles immobilized on modified gold substrate. A polyclonal anti-*Escherichia coli* antibody was immobilized for specific (*E. coli*) and non-specific (*Lactobacillus*) bacteria detection. Detection limit with a good reproducibility of 10^4 and 10^3 cfu mL⁻¹ of *E. coli* bacteria has been obtained for the first biosensor and for the second one respectively. A refractive index variation below 5×10^{-3} due to bacteria adsorption is able to be detected. The refractive index of the multilayer structure and of the *E. coli* bacteria layer was estimated with a modeling software.

© 2010 Elsevier B.V. All rights reserved.

1. Introduction

The development of a rapid method for the detection of pathogenic microorganisms remains a challenge and an issue for ensuring food and environment safety. The food industry needs rapid methods for the detection of pathogenic bacteria. Biosensors are needed for the detection of disease-causing agents in food and water to ensure continued security of the nation's food supply. Amperometric, piezoelectric (PZ) and impedimetric biosensors have been developed for the detection of pathogenic bacteria in food and water [1–3]. Surface plasmon resonance (SPR) phenomenon was used for biosensor applications [1–4]. SPR wave is an electromagnetic wave propagating along a metal/dielectric interface. For SPR biosensor, most recent works are based on the use of the self-assembled techniques [5–7]. For the increase of the sensitivity of the developed biosensors, one proposed solution is the use of gold nanoparticles that have gained an increasing interest due to their special features, such as unusual optical, electronic properties and easy functionalization [8–10].

The goal of this proposed work is to develop an immunooptical biosensor for rapid detection of two bacteria, one gram negative (*Escherichia coli*) and one gram positive (*Lactobacillus*)

with low detection limit. For the increase of the sensitivity, gold nanoparticles was functionalized and immobilized on gold substrates. The results indicate that gold nanoparticles increase the surface area to volume ratio which induces an increased sensitivity and an improved detection limit relative to bulk gold. A modeling software was used for refractive index and thickness determination.

2. Experimental

2.1. Reagents and apparatus

The used antibody is “goat polyclonal IgG anti-*E. coli* (ab13627)” purchased from Abcam (UK, United Kingdom). A phosphate buffer solution (PBS) of $5 \mu\text{g mL}^{-1}$ of antibody with pH=7.2 was prepared. The used bacteria were *E. coli* K12 (gram negative) and *Lactobacillus fermentium* (gram positive) diluted in PBS (pH=7.2) and concentration stability over time has been controlled with OD (optical density) measurement. All other materials, including amine–thiol (cysteamine), acid–thiol (16-mercaptohexadecanoic acid) (Sigma–Aldrich), 1-ethyl-3-(3-(dimethylamino)-propyl) carbodiimide (EDC) (Aldrich), *N*-hydroxy succinimide (NHS) (Aldrich) and glutaraldehyde (GA) (Aldrich) were used as supplied. The buffer solution used was a (PBS) containing 140 mM NaCl, 2.7 mM KCl, 0.1 mM Na₂HPO₄, 1.8 mM KH₂PO₄, adjusted at pH 7. All reagents were of analytical grade and ultrapure water (resistance $\geq 18.2 \text{ M}\Omega \text{ cm}^{-1}$) produced using a Millipore Milli-Q system was used throughout.

* Corresponding author at: Nanotechnology Laboratory, INSAT, Centre Urbain Nord, 1080 Charguia Cedex, Tunisia. Tel.: +216 71 703 829; fax: +216 71 704 329.
E-mail address: aabdelghan@yahoo.fr (A. Abdelghani).

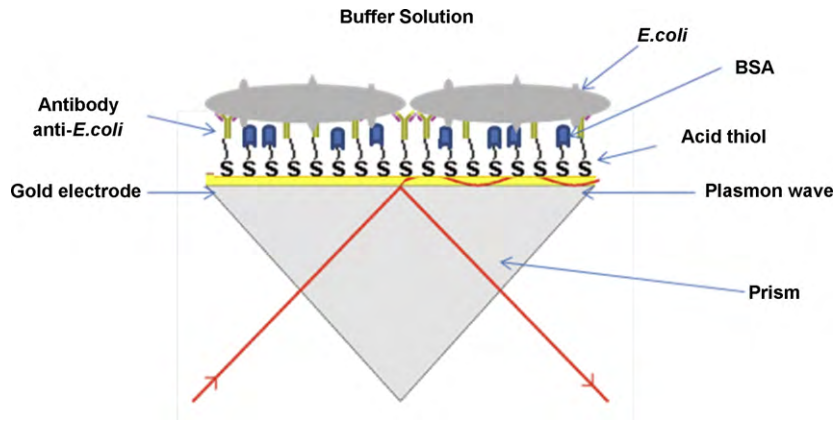


Fig. 1. SPR bacteria biosensor.

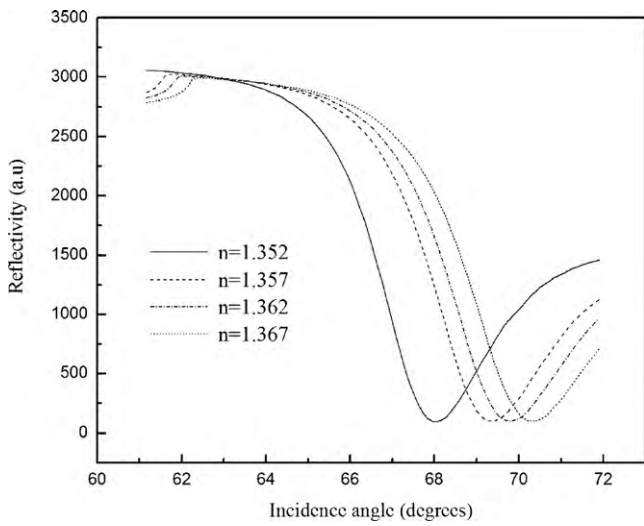


Fig. 2. SPR calibration curves for the gold substrates with different refractive index of the external medium.

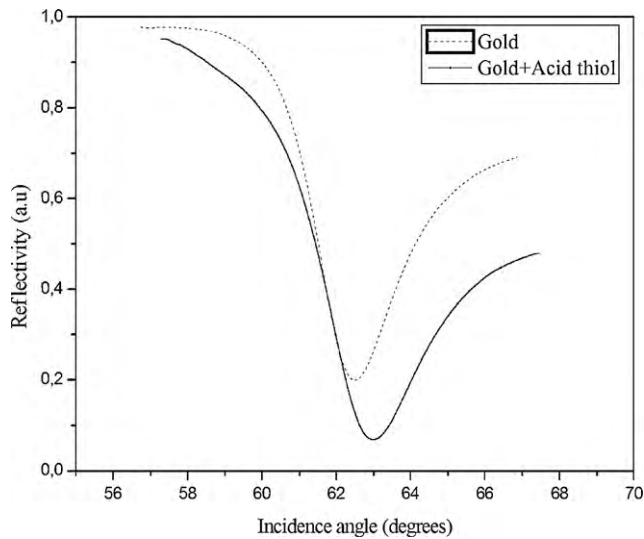


Fig. 3. Normalized reflectivity for gold and gold treated with acid-thiol as a function of the incidence angle.

2.2. Gold cleaning and functionalization

The gold substrates were cleaned in ethanol solution for 20 min. The substrates were immersed in a solution of 1 mM 16-mercaptoundecanoic acid (thiol acid) for 12 h for the obtaining of a dense self-assembled monolayer (SAM). The gold substrates were then rinsed with ethanol for removing the non-adsorbed acid-thiol. The terminal carboxylic group was converted to an active NHS

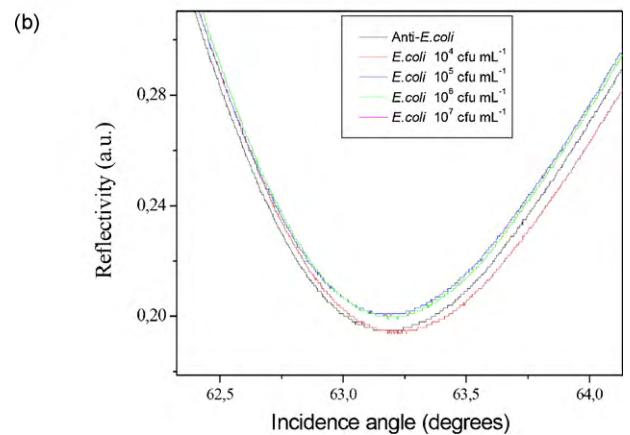
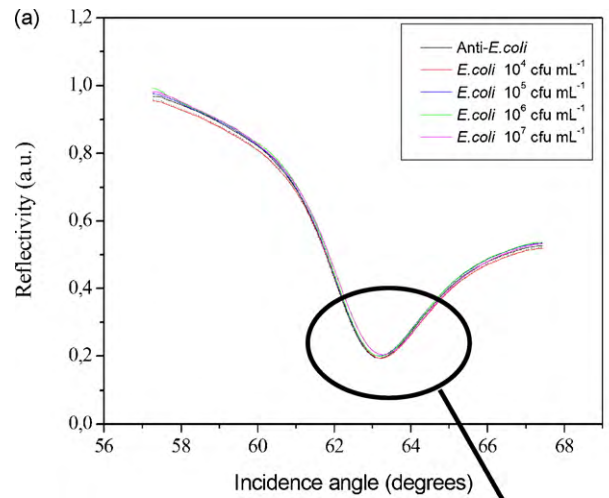


Fig. 4. Normalized reflectivity of biofunctionalized gold with immobilized antibody and with different concentrations of *E. coli* as a function of incidence angle.

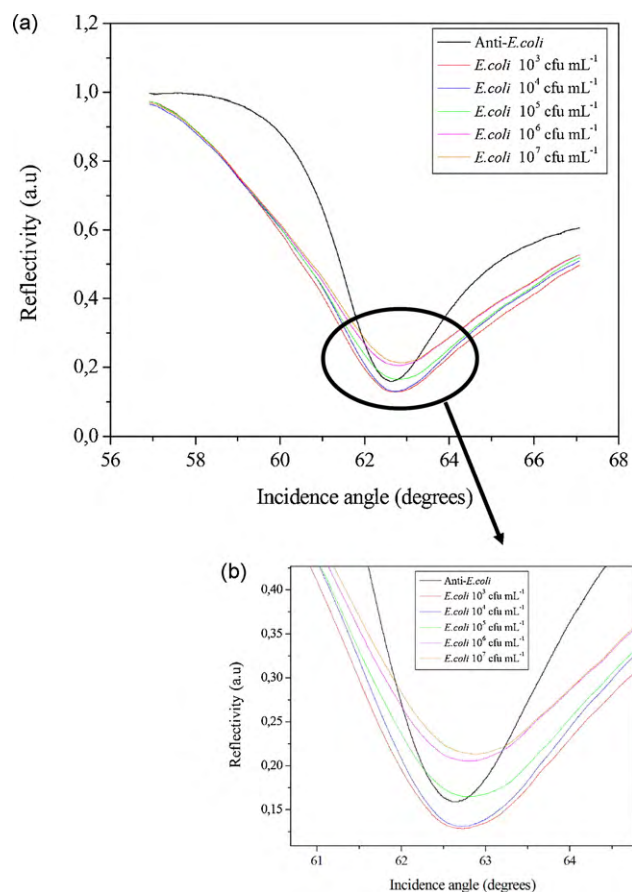


Fig. 5. Normalized reflectivity of biofunctionalized gold with immobilized gold nanoparticles for different concentrations of *E. coli* as a function of incidence angle.

ester through reaction with 0.4 mM EDC–0.1 mM NHS for 1 h. The gold substrates were then rinsed with PBS solution. A solution of 5 $\mu\text{g mL}^{-1}$ of polyclonal anti-*E. coli* IgG antibody was dropped onto the surface for 1 h at room temperature. The excess antibodies were removed by rinsing with PBS solution. Then, the antibody-modified substrates were treated with 0.1% BSA for 45 min, for blocking the non-specific sites (Fig. 1). After rinsing with PBS solution, the substrates were dried under nitrogen and were then ready to be used for bacteria detection.

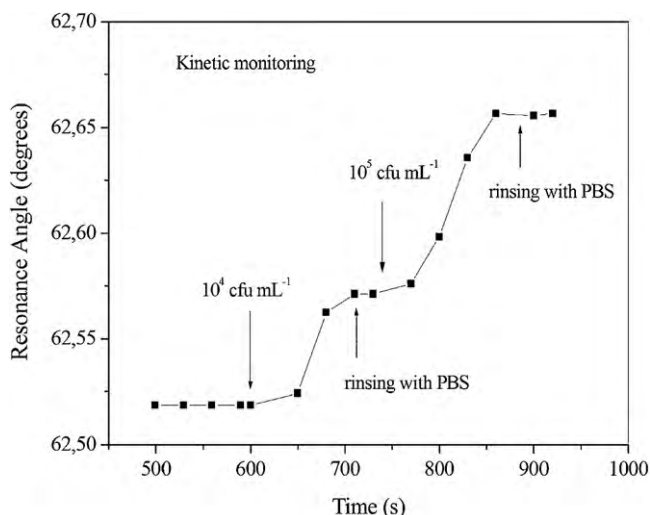


Fig. 6. Resonance angle variation versus time for different bacteria injections.

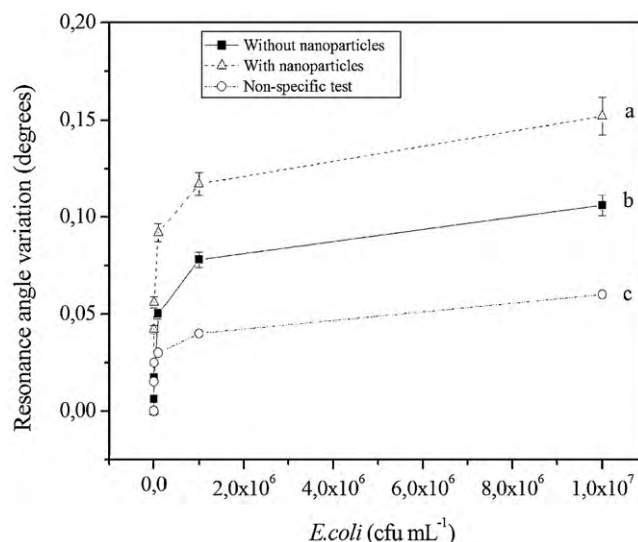


Fig. 7. Resonance angle variation versus the *E. coli* concentration without and with gold nanoparticles (a and b). (c) Non-specific test with gram positive bacteria.

2.3. Synthesis, functionalization and immobilization of gold nanoparticles

The gold nanoparticles were synthesized by the reduction of HAuCl_4 using sodium borohydride (NaBH_4). Briefly, 18.5 mL of deionized water, 0.5 mL of 0.01 mol L^{-1} sodium citrate and 0.5 mL of 0.01 M HAuCl_4 were placed in an Erlenmeyer flask and stirred for 3 min at 10°C . 0.5 mL of 0.01 mol L^{-1} NaBH_4 was slowly added to the reaction mixture and stirring was stopped immediately. The solution color changed from yellow to wine-red indicating formation of Au nanoparticles (6–8 nm size). The particles were centrifuged and the precipitate was redispersed in 0.01 mol L^{-1} aqueous sodium citrate solution. The concentration of the formed particles was $2.5 \times 10^{-4} \text{ mol L}^{-1}$ in sodium citrate solution. A volume of 100 μL of the nanoparticles solution was centrifuged and diluted (two times) in ultrapure water. A volume of amine-thiol (cysteamine) (1 mM) solution was added to the centrifuged nanoparticles. The mixture was left for 12 h at room temperature. The functionalized nanoparticles were then deposited on the acid-thiol treated substrate (which has been previously activated with EDC/NHS) for 1 h. The amine-thiol groups can be activated by immersing the substrate in PBS solution containing 5% (v/v) glutaraldehyde (GA) for 2 h. After rinsing with PBS, a $5 \mu\text{g mL}^{-1}$ solution of polyclonal anti-*E. coli* IgG antibody was added onto the surface for 1 h to achieve the base reaction between the aldehyde group of glutaraldehyde and the amino group of the antibody. Excess antibodies were removed by rinsing with PBS solution and the substrate was kept 45 min in 0.1% BSA solution for blocking the non-specific sites and any defect areas.

2.4. SPR instrumentation

The biomolecular immunoaffinity reactions were studied using SPR analyzer (Nano-SPR, USA) and gold-coated slides from the same company. The resolution of the resonance angle reading of the instrument is 0.003° with a maximal angle scan range of 17° . The SPR analyzer employed here is equipped with a flow system and dual channel. The SPR sensor was composed of prism (65° , F8 glass, refractive index 1.61, GaAs laser 650 nm), a microtube peristaltic pump and a flow cell. The gold slide ($10 \text{ mm} \times 10 \text{ mm} \times 1 \text{ mm}$) was matched to the prism using a refractive index matching liquid. A silicone flow cell of 10 mm thickness having a cylindrical cavity

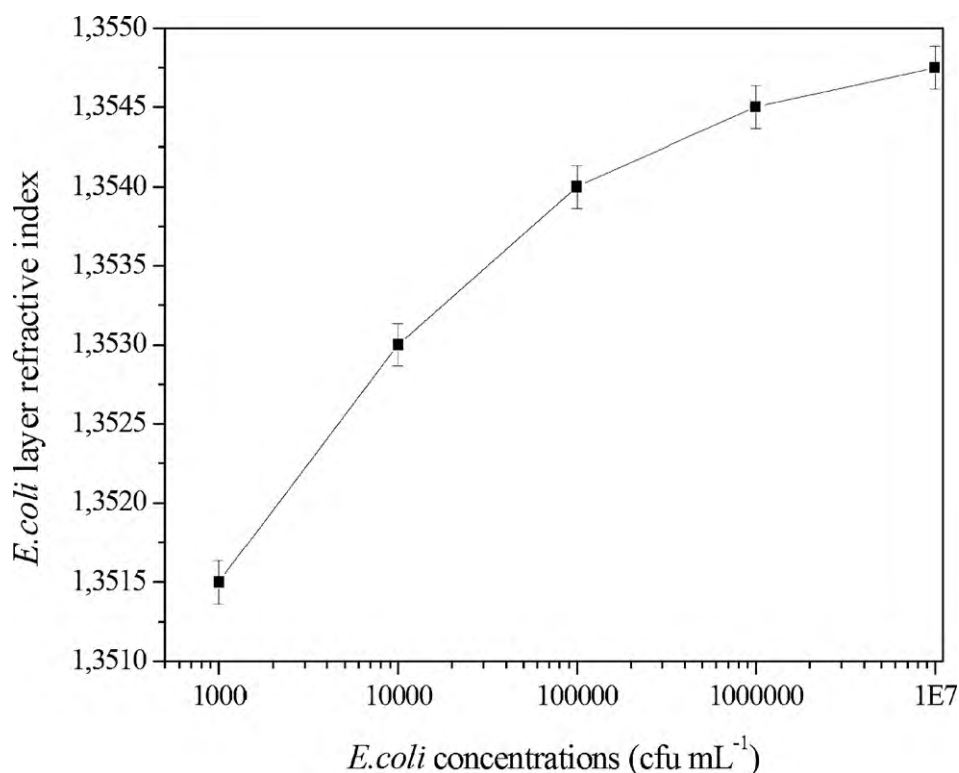


Fig. 8. Refractive index variation of *E. coli* layer versus *E. coli* concentrations.

(10 mm diameter and 50 μ l volume) was placed over the gold slide. Red light emitting from GaAs laser (2 mW, 650 nm) was reflected at the gold slide from the backside at attenuated total reflection angles, and the reflected light intensity was recorded as a function of the incident angle or of the time using a semiconductor photodiode. Four gold slides were used, one for calibration curve, the second one for thiol deposition and thickness estimation, the third one for bacteria detection with the self-assembled monolayers method, the fourth one for bacteria detection with gold nanoparticles. All the experiments were performed at a room temperature of 25 °C with sterile PBS solution.

3. Results and discussion

3.1. Calibration Curves

Fig. 2 shows the calibration curves which present the reflectivity variation versus the incidence angle for different refractive index of external medium. The variation of the resonance angle is due to the increase of the refractive index of the external medium. These curves show the shape of the minimum which gives information about the quality of the gold surface. A variation of 5×10^{-3} in refractive index can be easily detected as a variation in resonance angle. These curves were used for the assessment of the refractive index and of the thickness of the gold layer for the Winspall modeling software (Table 1). The Winspall program cannot be used without definition of the new gold constant (dielectric constant:

Table 1

Dielectric constant and thickness obtained through fitting of the experimental results using Winspall modeling software for the developed biosensor.

	Gold	Acid-thiol	Antibody + BSA	<i>E. coli</i>
Dielectric constant	$-16.67 + j 2.32$	2.308	2.25	-
Thickness	48.6 nm	1.14 nm	7 nm	0.8 μ m

$-16.67 + j 2.32$ and thickness: 48.6 nm). These values were slightly different from those obtained by other authors [11].

3.2. Thiol deposition

Fig. 3 shows the reflectivity variation versus the incidence angle for the gold and gold treated with acid-thiol (16-mercaptoundecanoic acid). The resonance angle changes from 62.47° to 63.01°. This shift is due to the adsorption of the thiol monolayer on the gold surface. The thickness and the refractive index of the thiol layer have been estimated using Winspall modeling software (Table 1).

3.3. *E. coli* detection using gold with SAM

Fig. 4 shows the reflectivity variation versus the incidence angle for the anti-*E. coli* antibody functionalized gold substrate after different injection of bacteria concentrations. The increase in the resonance angle is due to the specific recognition of bacteria with the antibody. A saturated signal has been obtained in the range of 10^5 – 10^7 cfu mL⁻¹. A limit detection of 10^4 cfu mL⁻¹ has been obtained with a good reproducibility.

3.4. *E. coli* detection using gold nanoparticles

Different concentrations of *E. coli* ranging from 10^3 to 10^7 cfu mL⁻¹ were tested using gold nanoparticles immobilized on gold surface.

Fig. 5 shows the reflectivity variation versus the incidence angle for different *E. coli* concentrations. The increase of *E. coli* concentration leads to that of resonance angle, due to the successful recognition of bacteria. A detection limit of 10^3 cfu mL⁻¹ has been obtained with a good reproducibility. Fig. 6 shows the resonance angle variation versus time for different bacteria injections. The signal increases due to bacteria interaction with the antibody,

then stabilizes. The response of the developed biosensor is about 1 min.

3.5. Sensitivity improvement and selectivity

The binding of bacteria to the functionalized gold surface is sensitively detected. Fig. 7 shows the induced resonance angle variation for different concentrations of bacteria without (Fig. 7a) and with gold nanoparticles (Fig. 7b). It shows a linear increase in the range of $0\text{--}10^5$ cfu mL⁻¹ and saturation behaviour in the range of $10^6\text{--}10^7$ cfu mL⁻¹. A detection limit of 10^3 cfu mL⁻¹ *E. coli* concentration was obtained with gold nanoparticles using a good reproducibility. This detection limit is smaller than those obtained without gold nanoparticles (10^4 cfu mL⁻¹). Thus, the results indicate that gold nanoparticles amplify the SPR signal. This effect can be due to the increase of the surface area to volume ratio and to collective oscillation of conduction electrons [12]. A negative test has been performed with *Lactobacillus* bacteria (gram positive). A very low signal has been obtained in comparison to the specific signal (Fig. 7c) obtained with *E. coli* using gold nanoparticles.

3.6. Modeling

Balaev et al. [13] worked on the refractive index determination of a water suspension of *Escherichia coli* K12 cells in the exponential phase of growth. The bacteria suspension is modeled as a system of randomly oriented homogeneous circular cylinders with identical radii and different lengths.

In this work, we fit the reflectivity curve for each bacteria concentration with Winspall software for the first biosensor (without nanoparticles). Fig. 8 shows the refractive index of *E. coli* bacteria layer obtained through fitting of the experimental data. The increase of the bacteria concentration induces an increase in the layer density, therefore an increase in the refractive index. The thickness of the bacteria layer was estimated to be 0.8 μm. The obtained refractive index values were slightly different from those obtained by other authors [13].

4. Conclusion

This work describes an approach for the development of two bacteria biosensors based on surface plasmon resonance (SPR) technique. The first biosensor was based on functionalized gold substrate and the second one was based on functionalized gold nanoparticles. For the first biosensor, the gold electrode was functionalized with thiol with the self-assembled monolayer technique, while the second one was functionalized with gold nanoparticles immobilized on modified gold substrate. The use of gold nanoparticles increases the surface area to volume ratio which induces an increased sensitivity and an improved detection limit. A negative test has been performed with *Lactobacillus* bacteria (gram positive).

Acknowledgments

The authors thank the Alexander Von Humboldt Foundation (Germany) for material donation and Pr. Sherine Obare (Michigan University, USA) for the collaboration.

References

- [1] A. Ghindilis, P. Atanasov, M. Wilkins, E. Wilkins, *Biosens. Bioelectron.* 13 (1998) 113.
- [2] J. Gau, E. Lan, B. Dunn, C. Ho, J. Woo, *Biosens. Bioelectron.* 16 (2001) 745.
- [3] A. Ishimaru, S. Jaruwatanadilok, Y. Kuga, *PIER* 51 (2005) 139.
- [4] J. Frischeisen, C. Mayr, N.A. Reinke, S. Nowy, W. Brütting, *Opt. Soc. Am.* 16 (2008) 18426.
- [5] M. Suzuki, F. Ozawa, W. Sugimoto, S. Aso, *Anal. Sci.* 17 (Suppl.) (2001).
- [6] P. Yanez-Sadeno, J.M. Pingarron, *Anal. Bioanal. Chem.* 382 (2005) 884.
- [7] S. Helali, H. Ben Fredj, K. Cherif, A. Abdelghani, C. Martelet, N. Jaffrezic-Renault, *Mater. Sci. Eng. C: Biomim. Mater. Sens. Syst.* 28 (2008) 588.
- [8] S.D. Mazumdar, B. Barlen, P. Kämpfer, M. Keusgen, *Biosens. Bioelectron.* 25 (2010) 967.
- [9] S.D. Mazumdar, M. Hartmann, P. Kämpfer, M. Keusgen, *Biosens. Bioelectron.* 22 (2007) 2040.
- [10] M. Geneviève, C. Vieu, R. Carles, A. Zwick, G. Brière, L. Salomé, E. Trévisiol, *Microelectron. Eng.* 84 (2007) 1710.
- [11] I. Hafaid, A. Gallouz, W.M. Hassen, A. Abdelghani, Z. Sassi, F. Bessueille, N.J. Renault, *J. Sensors* (2009) 12, Article ID 746548.
- [12] P. Banerjee, D. Conklin, S. Nanayakkara, T.H. Park, M.J. Therien, D.A. Bonnell, *ACS Nano* 4 (2) (2010) 1019.
- [13] A.E. Balaev, K.N. Dvoretzki, V.A. Doubrovski, *Proc. SPIE* 5068 (2003) 375.